Human Molecular Genetics, 2015, Vol. 24, No. 11 3238–3247

doi: 10.1093/hmg/ddv074
Advance Access Publication Date: 26 February 2015
Original Article

ORIGINAL ARTICLE

Complex I assembly function and fatty acid oxidation enzyme activity of ACAD9 both contribute to disease severity in ACAD9 deficiency

Manuel Schiff[1,2,*], Birgit Haberberger[3,4], Chuanwu Xia[5], Al-Walid Mohsen[1], Eric S. Goetzman[1], Yudong Wang[1], Radha Uppala[1], Yuxun Zhang[1], Anuradha Karunanidhi[1], Dolly Prabhu[1], Hana Alharbi[1], Edward V. Prochownik[1], Tobias Haack[3,4], Johannes Häberle[6], Arnold Munnich[7], Agnes Rötig[7], Robert W. Taylor[8], Robert D. Nicholls[1,9], Jung-Ja Kim[5], Holger Prokisch[3,4] and Jerry Vockley[1,9,*]

[1]Department of Pediatrics, University of Pittsburgh School of Medicine, University of Pittsburgh, Children's Hospital of Pittsburgh of UPMC, Pittsburgh, PA 15224, USA, [2]Reference Center for Inborn Errors of Metabolism, Hôpital Robert Debré, APHP, INSERM U1141 and Université Paris-Diderot, Sorbonne Paris Cité, Paris, France, [3]Institute of Human Genetics, Technische Universität München, Munich, Germany, [4]Institute of Human Genetics, Helmholtz Zentrum München, German Research Center for Environmental Health, Neuherberg, Germany, [5]Department of Biochemistry, Medical College of Wisconsin, Milwaukee, WI 53226, USA, [6]Division of Metabolism, University Children's Hospital Zurich, Zurich, Switzerland, [7]Institut Imagine and INSERM U781, Sorbonne Paris Cité, Hôpital Necker-Enfants Malades, APHP, Université Paris-Descartes, Paris, France, [8]Wellcome Trust Centre for Mitochondrial Research, The Medical School, Newcastle University, Newcastle upon Tyne, UK and [9]Department of Human Genetics, University of Pittsburgh, Pittsburgh, PA 15224, USA

*To whom correspondence should be addressed at: Reference Centre for Inborn Errors of Metabolism, Robert Debré University Hospital, 48, Bd Sérurier, 75935 Paris Cedex 19, France. Tel: +33 140035707; Fax: +33 1 40034774; Email: manuel.schiff@rdb.aphp.fr (M.S.); Department of Pediatrics, University of Pittsburgh School of Medicine, Children's Hospital of Pittsburgh of UPMC, Pittsburgh, PA 15224, USA. Email: vockleyg@upmc.edu (J.V.).

Abstract

Acyl-CoA dehydrogenase 9 (ACAD9) is an assembly factor for mitochondrial respiratory chain Complex I (CI), and *ACAD9* mutations are recognized as a frequent cause of CI deficiency. ACAD9 also retains enzyme ACAD activity for long-chain fatty acids *in vitro*, but the biological relevance of this function remains controversial partly because of the tissue specificity of ACAD9 expression: high in liver and neurons and minimal in skin fibroblasts. In this study, we hypothesized that this enzymatic ACAD activity is required for full fatty acid oxidation capacity in cells expressing high levels of ACAD9 and that loss of this function is important in determining phenotype in ACAD9-deficient patients. First, we confirmed that HEK293 cells express ACAD9 abundantly. Then, we showed that *ACAD9* knockout in HEK293 cells affected long-chain fatty acid oxidation along with Cl, both of which were rescued by wild type *ACAD9*. Further, we evaluated whether the loss of ACAD9 enzymatic fatty acid oxidation affects clinical severity in patients with *ACAD9* mutations. The effects on ACAD activity of 16 *ACAD9* mutations identified in 24

Received: November 27, 2014. **Revised and Accepted:** February 23, 2015

patients were evaluated using a prokaryotic expression system. We showed that there was a significant inverse correlation between residual enzyme ACAD activity and phenotypic severity of ACAD9-deficient patients. These results provide evidence that in cells where it is strongly expressed, ACAD9 plays a physiological role in fatty acid oxidation, which contributes to the severity of the phenotype in ACAD9-deficient patients. Accordingly, treatment of ACAD9 patients should aim at counteracting both CI and fatty acid oxidation dysfunctions.

Introduction

The acyl-CoA dehydrogenases (ACADs) are a family of flavoenzymes that catalyze the first step of fatty acid β-oxidation (FAO) in mitochondria (1). Acyl-CoA dehydrogenase 9 (ACAD9) deficiency was originally described in three patients who had variable disease phenotypes but shared aspects compatible with FAO disorders (2). All three exhibited either absent or markedly reduced ACAD9 protein and/or mRNA, with normal mitochondrial respiratory chain activities in muscle for the one patient studied; however, the mutational basis for the defect in 2/3 cases was not identified. Subsequently, three studies of patients with isolated mitochondrial respiratory chain complex I (CI) deficiency identified recessive mutations in the *ACAD9* gene (3–5). These mutations were shown to affect CI assembly without biochemical evidence of FAO dysfunction in either blood or fibroblasts. Several additional cases of isolated CI deficiency associated with recessive *ACAD9* point mutations have since been reported (6–10).

While ACAD9 has an unambiguous role in CI assembly, the biological relevance of its function as a FAO enzyme has been controversial. We previously showed that ACAD9 has broad substrate specificity for acyl-CoAs *in vitro* (11). It has recently been demonstrated that ACAD9 contributes to the accumulation of C14:1-carnitine in very long-chain acyl-CoA dehydrogenase (VLCAD)-deficient patient skin fibroblasts, and minimally to whole-cell FAO (12). However, the physiologic role of ACAD9 remained questionable, as its reduction in normal fibroblasts increased whole-cell FAO. In contrast, ACAD9 has been suggested to be a major contributor to FAO in tissues where it is highly expressed, such as the liver and central nervous system (2). In the present work, we hypothesized that the ACAD function of ACAD9 is required for full FAO capacity in cell types where it is abundantly expressed and, moreover, that the loss of this FAO function contributes to the pathophysiology of ACAD9 deficiency. To test this hypothesis, we followed three approaches. First, we used transcription activator-like effector nuclease (TALEN) technology to knockout *ACAD9* in HEK293 cells, which normally express abundant ACAD9, and measured FAO and CI activities. Second, we studied FAO in fibroblasts from *Acadl*/*Acadvl* double-knockout mice. Finally, we expressed *ACAD9*-mutant alleles identified in patients with CI deficiency in a prokaryotic system and analyzed the ACAD activity of the recombinant proteins.

Results

ACAD9 knockout affects long-chain fatty acid oxidation

ACAD9 expression varies across tissues, with particularly high expression in brain and liver. HEK293 cells derive from embryonic kidney but have been shown to have characteristics in common with neurons (13,14), and they express high levels of *ACAD9* (Supplementary Material, Fig. S1A and B) as compared with skin fibroblasts. To further characterize the physiological contribution of ACAD9 to FAO, we generated *ACAD9*-deficient HEK293 cells in which mutations were established in exon 2 of *ACAD9* by non-homologous end-joining repair of a TALEN-induced double-strand break (Supplementary Material). Two clonal cell lines lacking expression of ACAD9 were evaluated. Clone A had a single allele harboring a complex mutation comprising a 62-bp deletion including intron 1 and exon 2 sequences of *ACAD9*, along with a 102-bp insertion (Supplementary Material). Clone B had a 22-bp deletion that created a frameshift in one allele, and a 15-bp in-frame deletion in the other allele (Supplementary Material). We confirmed that ACAD9 protein was not detectable in these cells whereas VLCAD and MCAD (medium-chain acyl-CoA dehydrogenase) protein levels were not affected (Fig. 1A). Whole-cell mitochondrial palmitate oxidation, defined as etomoxir-sensitive degradation of ^{3}H-palmitate, and specific ACAD activity for palmitoyl-CoA were measured in the two *ACAD9* –/– clonal cell lines. As shown in Figure 1B, both cell lines exhibited a 35–40% decrease in whole-cell palmitate oxidation and palmitoyl-CoA ACAD activity, thereby confirming that ACAD9 normally plays a role in long-chain FAO in HEK293 cells. Conversely, octanoate oxidation was unaffected (Fig. 1C), indicating that the decrease in palmitate oxidation was not merely a secondary effect of the defective CI assembly (Fig. 2A and B). Additionally, evolutionary conserved signaling intermediate in toll pathways (ECSIT), a binding partner in ACAD9-mediated CI assembly, was absent in both ACAD9-deficient cell lines (Fig. 2B). Also, we verified that both the CI and long-chain FAO defects were attributable to loss of ACAD9 activity by re-introducing a wild type *ACAD9* cDNA back into *ACAD9*-deficient clone A and restoring ACAD9 expression. Immunostaining verified that the wild type ACAD9 protein was expressed at normal levels and properly targeted to mitochondria (Fig. 3A). We then confirmed complete rescue of long-chain FAO (Fig. 3B) as well as the presence and activity of CI and ECSIT protein (Fig. 3C).

ACAD9 can oxidize long-chain fatty acids in mouse fibroblasts

To evaluate the role of ACAD9 in another mammalian model, we studied fibroblasts from *Acadl*/*Acadvl* double-knockout mice. These animals typically die shortly after birth, most likely as a result of hypothermia and hypoglycemia, thereby mimicking severe (and usually fatal) neonatal onset human FAO disorders (Keith Cox, personal communication) (15). The only persisting long-chain FAO enzyme was ACAD9 (Fig. 4A). In contrast to human VLCAD-deficient fibroblasts, these mouse fibroblasts deficient in LCAD and VLCAD displayed ~50% residual long-chain FAO [residual palmitate oxidation rate (Fig. 4B) and palmitoyl-CoA ACAD activity (Fig. 4C)] consistent with a physiologic role for ACAD9 in FAO in these cells.

Phenotypic severity of ACAD9-deficient patients is correlated with residual enzyme ACAD activity

To study the impact of mutations in *ACAD9* on ACAD9 stability and enzyme function, we selected 16 *ACAD9* alleles with point mutations [previously reported or recently identified in 24 CI-deficient patients (Supplementary Material, Table S1)] and studied them in an *Escherichia coli* expression system (Fig. 5). First, we

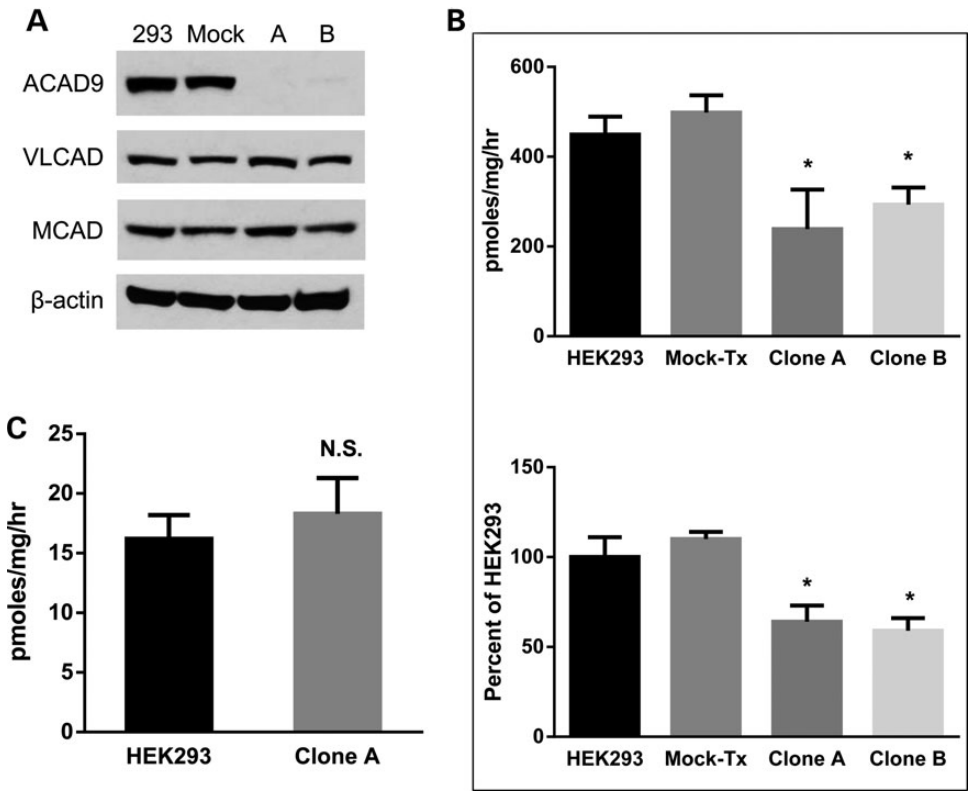

Figure 1. Targeted gene disruption of *ACAD9* in HEK293 cells selectively affects long-chain FAO and not medium-chain FAO. (**A**) Cell lysates from HEK293 cells (293), mock-treated HEK293 cells (Mock) and two *ACAD9* –/– cell clones derived from TALEN-transfected cells (clones A and B both with *ACAD9*-null mutations) were subjected to SDS–PAGE and western blotting with the indicated antibodies. β-actin was used as control. (**B**) Etomoxir-sensitive palmitate oxidation rate (top) and palmitoyl-CoA dehydrogenase activity (bottom) were determined in HEK293, mock-treated (Mock-Tx) and the two *ACAD9* –/– clones (clones A and B). All values are presented as average ± SD ($n = 4$ for each condition); $^*P < 0.05$. (**C**) Octanoate oxidation rates were determined in HEK293 cells and TALEN-mediated *ACAD9* –/– clone A. All values are presented as average ± SD ($n = 4$). N.S., not significant.

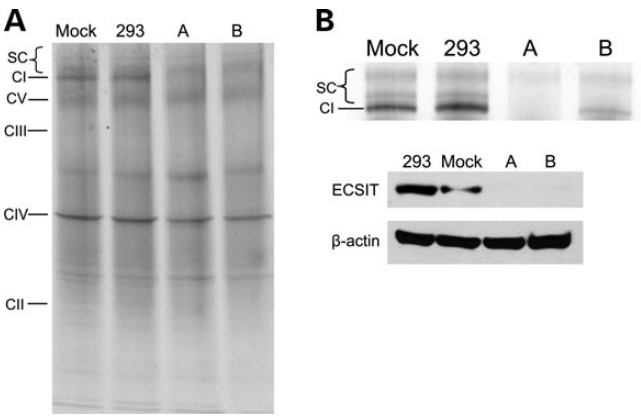

Figure 2. Targeted gene disruption of *ACAD9* in HEK293 cells affects formation of supercomplexes (**A**) as well as CI activity and ECSIT binding (**B**). (A) Mitochondria isolated from HEK293, mock-treated HEK293 and the two *ACAD9* –/– clones A and B were permeabilized with digitonin and resolved by BNGE (Blue Native Gel Electrophoresis) followed by Coomassie Blue staining to visualize individual respiratory chain complex bands (CI to IV) and supercomplexes (SC). (B) Top: BNGE analysis of CI in-gel activity was performed in isolated mitochondria from HEK293, mock-treated HEK293 and the two *ACAD9* –/– clones A and B. Bottom: SDS–PAGE immunodetection of ECSIT and β-actin in cell lysates from the same cell lines.

analyzed ACAD9 stability and enzymatic activity in crude bacterial extracts. Second, we purified the mutant recombinant ACAD9 proteins to study their trypsin sensitivity used as an indicator of stability/folding. Finally, ACAD activity of the recombinant purified proteins was analyzed. Western blot on cell lysates with an anti-ACAD9 antibody showed lower levels of ACAD9 antigen for nine mutations and levels comparable with non-mutated ACAD9 for seven (R266Q, E413K, R417C, R469W, R518H, R532Q and R532W). For eight alleles, the mutations were effectively null, with no detectable dehydrogenase activity (I87N, R127Q, A220V, R266Q, A326P, E413K, R417C and D418G). Of the remaining eight mutant proteins, two (R532Q and R532W) exhibited ACAD9 activity indistinguishable from wild type; four (F44I, R469W, R518C and R518H) had mildly decreased activity (70–80% compared with wild type ACAD9) and two (L98S and R433Q) exhibited low activity (15–20% of wild type ACAD9) (Fig. 5A).

Studies on the recombinant ACAD9 his-tagged purified proteins largely reflected the results obtained with crude extracts. The mutants found inactive in the crude extracts were all trypsin hypersensitive (i.e. poorly folded) except for R127Q, and enzymatically inactive when purified (Fig. 5B and Supplementary Material, Fig. S2). Conversely, the mutants that were stable and active in the crude extracts were resistant to trypsin digestion and active when purified (Fig. 5B and Supplementary Material, Fig. S2). ACADs purified following prokaryotic expression often lose an essential FAD cofactor, resulting in a decrease in measured enzyme activity that can be restored by incubation with excess FAD. The trypsin digestion patterns of ACAD9 recombinant mutant proteins with 20× added FAD are similar to those without FAD (not shown), and this stability correlated well with their activities after FAD addition (Fig. 5C and Supplementary Material,

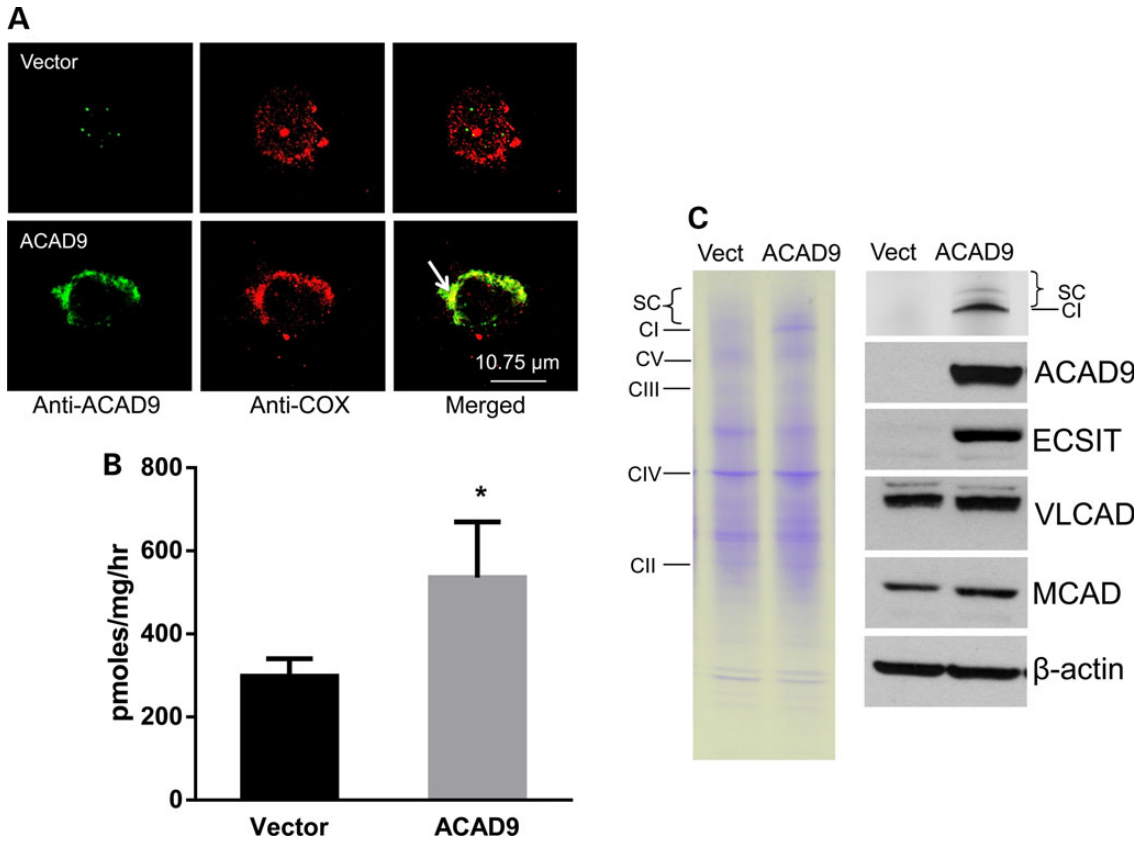

Figure 3. Long-chain FAO and CI defects are restored in *ACAD9*-deficient cells by transfection of an *ACAD9* expression vector. (**A**) Re-expression of *ACAD9* in *ACAD9* –/– HEK293 clone A cells transfected with empty pcDNA3.1 vector (Vect) or pcDNA-ACAD9 (ACAD9). The ACAD9 antigen was visualized with green fluorescently tagged antibodies, and mitochondrial cytochrome c oxidase (COX) was visualized with red fluorescently tagged antibodies. The merged image (arrow) shows co-localization of ACAD9 and COX in mitochondria as yellow. Scale bar, 10.75 μm. (**B**) Etomoxir-sensitive palmitate oxidation rates were determined in pcDNA3.1 (Vect) and pcDNA-ACAD9 (ACAD9) transfected clone A. Values are presented as average ± SD ($n = 4$); *$P < 0.05$. (**C**) Left panel: mitochondria isolated from TALEN-mediated ACAD9-deficient HEK293 clone A transfected with pcDNA3.1 vector (Vect) or pcDNA-ACAD9 (ACAD9) were permeabilized with digitonin and resolved by BNGE followed by Coomassie Blue staining to visualize individual respiratory chain complex bands (CI to IV) and supercomplexes (SC). Right: BNGE analysis of CI in-gel activity was performed in isolated mitochondria from pcDNA3.1-transfected (Vect) and pcDNA-ACAD9-transfected (ACAD9) clone A (top). Cell lysates from these two cell lines were subjected to SDS–PAGE and western blotting with the indicated antibodies. β-actin was used as control.

Fig. S2). Activity of the purified enzymes after addition of excess FAD also correlated well with ACAD9 activity in crude bacterial extracts.

Thus, while all 16 alleles were found in patients with CI deficiency, ACAD enzyme activity of mutant proteins varied from non-detectable to normal levels and thus did not correlate with the CI defect. This demonstrates that mutations in *ACAD9* lead to CI deficiency independent of their effects on ACAD enzyme activity.

Next, we used molecular modeling of the *ACAD9* point mutations to identify their locations in the enzyme structure. Among the ACADs, ACAD9 is structurally closest to VLCAD; both of them have an extended C-terminal domain that has been linked with inner mitochondrial membrane association (11,16,17). The atomic coordinates of VLCAD [PDB: 3B96, (18)] were therefore used to predict the ACAD9 3D structure and investigate the impact of the mutations on structure and/or function (Fig. 6). Mutations with little or no impact on ACAD activity were all observed to be located in the C-terminal domain of the protein. In contrast, the inactivating mutations were all localized to the catalytic portion of the molecule, which is conserved in all mitochondrial matrix ACADs including those that lack the membrane interacting domain.

Patients with CI deficiency caused by *ACAD9* mutations display a broad range of clinical severity. We therefore asked whether the dehydrogenase enzyme activity detected in the ACAD9 prokaryotic expression system correlated with the severity of the clinical phenotype. We used the mean of both alleles' enzyme activity, a generally accepted surrogate of *in vivo* activity when modeling genotype–phenotype correlation in recessive inborn errors of metabolism (19,20). Clinical phenotypes were classified into two degrees of severity, mild or severe. Mild phenotype (severity score = 1) was defined as exercise intolerance and/or cardiomyopathy, whereas severe phenotype (severity score = 2) included encephalopathy and/or death before 2 years of age (Supplementary Material, Table S1). In two families with two affected siblings, the index patient died within the first 2 years of life (Score 2) whereas the second affected patient had a much less severe clinical course (Score 1). In both cases, only the second child was preventatively treated with riboflavin, which increased residual CI activity in patient-derived cell lines (3), and may have impacted clinical outcome (4) (Supplementary Material, Table S1). Therefore, only index cases were included in the analysis. Logistic regression analysis revealed that the mean of both alleles' ACAD9 dehydrogenase activity as determined in the prokaryotic expression system significantly predicted clinical severity ($P = 0.034$, estimate −0.034, SE = 0.016, Nagelkerke pseudo $R^2 = 0.314$). Conversely, and as previously reported (6,21–23), CI activity was not found to be a significant predictor of clinical

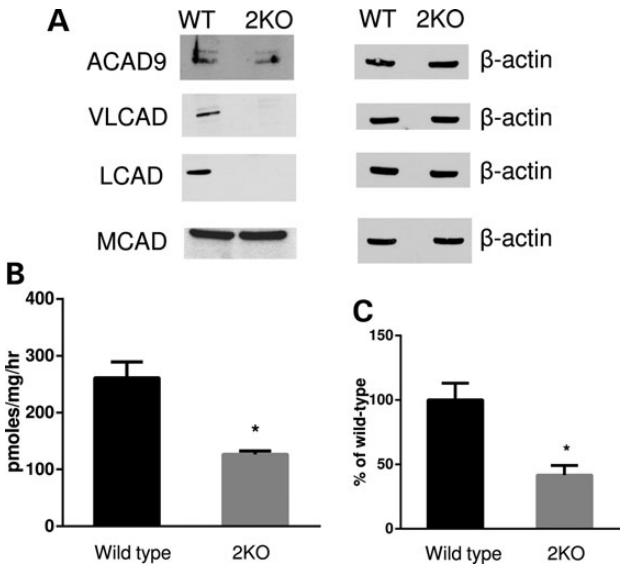

Figure 4. Mouse double-knockout *Acadl* –/–, *Acadvl* –/– (2KO) neonatal fibroblasts exhibit residual long-chain FAO capacity. (**A**) Cell lysates from wild type (WT) and double-knockout mouse fibroblasts (2KO) were subjected to SDS–PAGE and western blotting with the indicated antibodies. β-actin was used as control. Etomoxir-sensitive palmitate oxidation rates (**B**) and palmitoyl-CoA dehydrogenase activity (**C**) were determined in WT and 2KO double-knockout mouse fibroblasts. Values are presented as average ± SD ($n = 4$); *$P < 0.05$.

severity in fibroblasts ($P = 0.08$, estimate –0.06, SE = 0.035, Nagelkerke pseudo $R^2 = 0.34$) or skeletal muscle ($P = 0.616$, estimate 0.012, SE = 0.024, Nagelkerke pseudo $R^2 = 0.024$).

Discussion

Using three model systems (human knockout cells, mouse fibroblasts and recombinant mutants in prokaryotic cells), we provide evidence that in cells where it is strongly expressed, ACAD9 plays a physiological role in fatty acid oxidation that is independent of its function as a CI assembly factor. Furthermore, the level of residual ACAD activity contributes to the severity of the clinical phenotype in ACAD9-deficient patients. In cell types such as HEK293 (derived from an embryonic kidney peripheral neuronal precursor cell (13) and expressing ACAD9 abundantly) or neonatal mouse fibroblasts, the ACAD9 protein is utilized for both CI assembly and FAO. Consistent with this observation, the residual ACAD9 protein seen following RNAi-mediated *ACAD9* knockdown in HEK293 cells was previously shown to be sufficient to maintain a normal long-chain FAO rate but impacted CI assembly (5). Similarly, *ACAD9* knock down in VLCAD-deficient human fibroblasts affects the very low residual FAO activity, whereas over expression of an inactive ACAD9 protein rescues CI activity (12). Both functional roles should also be important in liver in which ACAD9 and VLCAD equally contribute to long-chain FAO (2). In contrast, other human tissues such as muscle or heart express only small amounts of ACAD9 protein relative to VLCAD. They contain enough protein to mediate CI assembly function without contributing appreciably to FAO. While the role of FAO in the brain is not understood, ACAD9 is the only long-chain ACAD enzyme expressed there (2) and is especially abundant during fetal life (24,25). It is therefore tempting to speculate that a deficiency in brain FAO contributes to the neurological symptoms present in the most severely affected ACAD9-deficient patients. This notion is supported by our finding that ACAD9-deficient patients exhibiting neurological symptoms tended to have *ACAD9* mutations that either abolish or greatly reduce the protein's dehydrogenase activity. Similarly, robust expression of ACAD9 in the fetal brain might explain why our attempt to generate homozygous knockout *Acad9* mice was unsuccessful, with embryonic lethality presumably being attributable to a severe combined defect in both ACAD9 functions (unpublished data). Substantial ACAD9 expression in the nervous system might also compensate a VLCAD defect and explain the absence of neurological involvement in VLCAD-deficient patients (26). Thus, human ACAD9 deficiency should be viewed as a bifunctional disorder in mitochondrial energy metabolism (12) with an additional phenotypic burden in the patients bearing mutations that affect both CI assembly as well as long-chain FAO.

The molecular modeling described herein offers some insights into the underlying mechanisms by which different *ACAD9* mutations mediate their pathologic effects. *ACAD9* mutations that preserved enzyme activity are located in the 176 amino acid C-terminal domain. In VLCAD, the corresponding C-terminal domain interacts with inner mitochondrial membrane components, whereas its catalytic domain mediates the interaction with the rest of a fatty acid complex (27,28). The C-terminus of ACAD9 likely interacts with a different molecular partner(s) than its equivalent in VLCAD. Rather, we hypothesize that it serves to interact with the mitochondrial inner membrane, ECSIT, TMEM126B or CI intermediates (29). This is consistent with the observation that mutations in the C-terminal domain of ACAD9 affect CI assembly without impairing ACAD catalytic activity. As ACAD9 is not highly expressed in human fibroblasts, it is not possible to directly demonstrate the effect of the C-terminal *ACAD9* mutations on FAO. However, we speculate that they will retain at least some FAO activity in liver and neurons. In contrast, mutations affecting ACAD9 enzyme function were all localized to the ACAD catalytic domain, where they disrupt both catalytic activity and CI assembly functions owing to more broad effects on enzyme folding and/or stability. Such global perturbation in enzyme structure is consistent with previous findings regarding the effect of mutations, especially those at the FAD binding site, on other ACADs (30–39).

Our findings suggest that treatment of the long-chain FAO defect introduced by some *ACAD9* mutations with interventions such as avoidance of fasting, medium-chain triglycerides (40) or triheptanoin anaplerotic therapy (41) should be helpful to optimize long-term outcome in patients. Interestingly, riboflavin has been reported to improve muscle function and exercise tolerance in some ACAD9-deficient patients (4) but not in others (9). Riboflavin is the precursor for the FAD cofactor that is essential for ACAD enzyme activity and stability (42). Therefore, riboflavin responsiveness in ACAD9-deficient patients (4) may be related to a direct increase of the ACAD activity. In addition, it may also stabilize the protein so as to allow a more efficient CI assembly (3).

The recognition of mitochondrial enzymes with dual functions is growing, and in keeping with our findings on ACAD9, the moonlighting function may be non-enzymatic. For example, HSD10 operates as an enzyme in catabolism of the branched chain amino acid isoleucine (43) but is also one of three protein components of mitochondrial RNaseP that is required for mitochondrial integrity and cell survival (44). Similarly, short-chain 3-hydroxyacyl-CoA dehydrogenase is an enzyme involved in short-chain FAO, but the major clinical consequences of its deficiency are due to its moonlighting inhibitory function on glutamate dehydrogenase enzymatic activity in pancreatic β-cells (45). Loss of this non-enzymatic function leads to increased

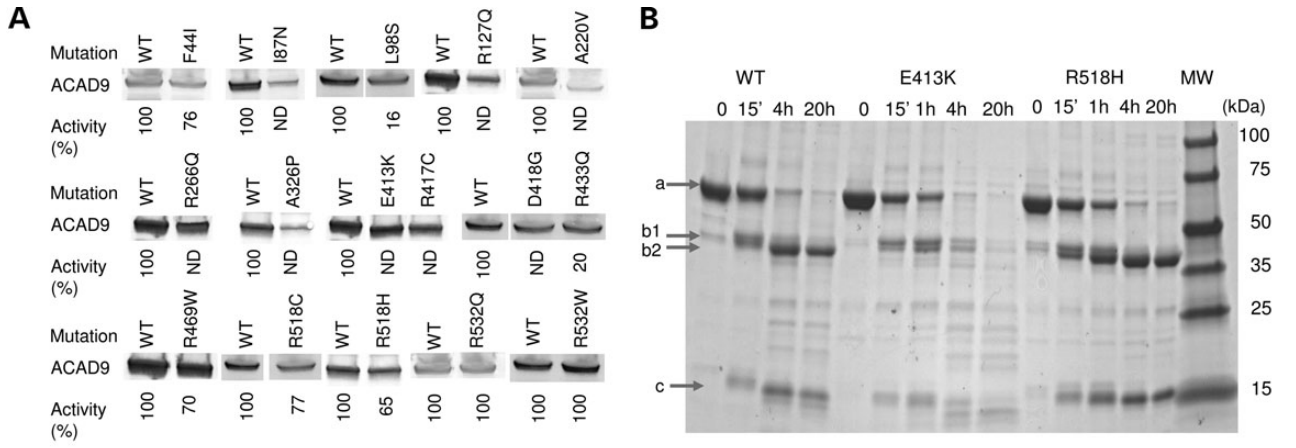

C

	WT	F44I	I87N	L98S	R127Q	A220V	R266Q	A326P	E413K	R417C	D418G	R433Q	R469W	R518C	R518H	R532Q	R532W
S	+++	++	+	+	+	-	+++	+	+++	+++	+	++	+++	+++	+++	+++	+++
T	+++	NA	-	++	+	NA	-	-	-	-	-	+	++	NA	+++	NA	+++
C	100	76	ND	16	ND	ND	ND	ND	ND	ND	ND	20	70	77	65	100	100
P	1.7	NA	ND	1.1	0.77	NA	0.2	ND	ND	ND	ND	0.22	1.40	NA	1.47	NA	1.56
%	100	NA	ND	68	45	NA	12	ND	ND	ND	ND	13	82	NA	87	NA	92

Figure 5. *ACAD9* missense mutations affect FAO independent from its CI assembly function. (**A**) Prokaryotic mutagenesis and expression studies of 16 *ACAD9* alleles containing missense variants. Each allele with the predicted amino acid substitution shown at the top of the figure was expressed in *E. coli*, and the cell-free extract was analyzed by SDS–PAGE followed by western blotting with anti-ACAD9 antibodies (middle). Palmitoyl-CoA dehydrogenase activity (ACAD9 activity) in cell-free extracts following prokaryotic expression is given on the bottom line. ND: non-detectable. ACAD9 activity of each mutant protein is expressed as % of the activity of wild-type (WT) ACAD9 expressed in *E. coli*. (**B**) SDS–PAGE analysis of recombinant wild type-His-tagged ACAD9 (WT) and two mutants ACAD9 proteins chosen as an example (E413K, unstable and R518H, stable) during limited trypsin digestion. The molar ratio of protein to trypsin was 1000:1. The reactions were initiated by adding trypsin into 1 mg/ml ACAD9 proteins in 25 mM sodium phosphate buffer, pH 7.6, containing 100 mM NaCl and 10% glycerol. Aliquots were taken at indicated times for SDS–PAGE analysis. While band **a** represents the entire mature ACAD9 peptide (65 kDa), the molecular weight of bands **b** and **c** correspond to the N-terminal domain (45 kDa) and C-terminal domain (17 kDa) of the mature ACAD9 protein, respectively. Bands **b1** and **b2** correspond to an additional cleavage site in the loop region connecting N-terminal and C-terminal domain. Upon addition of trypsin, both WT, E413K and R518H mutants are quickly digested into two pieces: the N-terminal domain (45 kDa) and the C-terminal domain (17 kDa). However, as the trypsin digestion continues, the N-terminal and C-terminal domains of E413K were further cleaved into smaller pieces (instability), whereas the two domains of WT and R518H are very stable. (**C**) Comparison between crude extracts (white) and purified protein data (gray) for each mutants. S: stability of the recombinant ACAD9 proteins from crude extracts evaluated on western blots (+++: very stable; –: very unstable). T: stability of the recombinant purified ACAD9 proteins after trypsin proteolysis (+++: very stable; –: very unstable). C: ACAD activity of crude extract. %: percentage of the activity of wild type recombinant ACAD9. P: specific activity of the recombinant purified ACAD9 expressed as μmole of C16-CoA oxidized/min/mg of ACAD9 protein in the presence of added FAD. NA: not available. ND: non-detectable. MW: molecular weight.

glutamate dehydrogenase activity, resulting in insulin secretion hypersensitivity. Other proteins associated with CI also have moonlighting functions. For example, NDUFAB1, a CI structural subunit, has an acyl carrier protein domain involved in fatty acid synthesis (46), and it has been suggested that some of the CI structural subunits may act as a molecular scaffold for as yet unrecognized enzymatic activities (47). Overall, the occurrence of mitochondrial enzymes with dual functions is likely to be of greater import than previously recognized. So far, in all identified patients with *ACAD9* mutations, the non-enzymatic function is impaired whereas the FAO activity might be an important factor in determining severity of phenotype. Better delineation of the interplay between these functions is central for understanding the clinical heterogeneity characteristic of many mitochondrial metabolic disorders.

Materials and Methods

Mutagenesis and expression studies

For prokaryotic mutagenesis studies, 16 *ACAD9* mutations (F44I, I87N, L98S, R127Q, A220V, R266Q, A326P, E413K, R417C, D418G, R433Q R469W, R518C, R518H, R532W and R532Q) were introduced into a pEThACAD9 expression plasmid (11) using the QuickChange Site-Directed Mutagenesis Kit according to the manufacturer's instructions (Agilent, Santa Clara, CA, USA). Mutations were verified by sequencing, and the plasmids were introduced into an *E. coli* expression strain (BL21), cultured at 37°C and induced for expression studies as previously described (27). Enzyme activity was determined using the ETF-fluorescence reduction assay and western blotting was performed on cell-free extracts as previously described (27,48,49). ACAD9 wild-

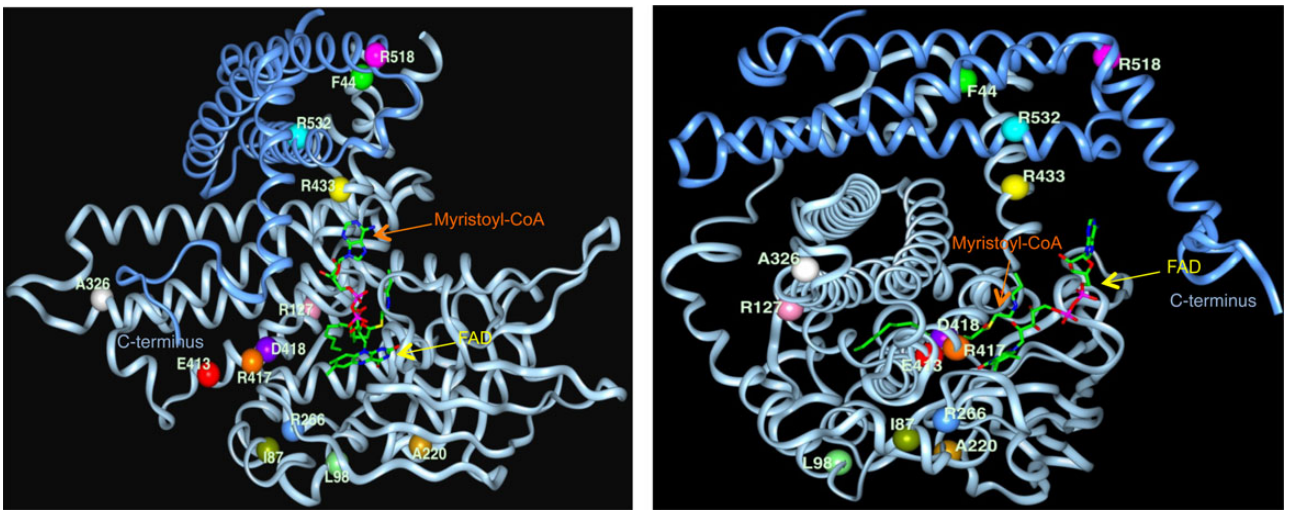

Figure 6. Molecular modeling of the *ACAD9* mutations. Two perpendicular views of ribbon representations of a human ACAD9 monomer model (11) showing the active site with bound FAD and the acyl moiety of myristoyl-CoA and the location of missense mutations found in ACAD9-deficient patients. The second monomer, hidden, lies between the C-terminus (blue) α-helix and the rest of the monomer (gray). The model was generated using the human VLCAD crystal structure coordinates (PDB: 3B96) (18). The peptide stretch 448–494 is not represented as its equivalent in the template molecule, the VLCAD crystal, is disordered.

type and mutant proteins with C-terminal His tag (GSHHHHHH) were similarly expressed and then purified on a His60 Ni resin column (Clontech, Mountain View, CA, USA) per the manufacturer's instructions. ACAD activity of the purified ACAD9 recombinant proteins was assayed using ferricenium as the final electron acceptor as described (50). Assays were performed both with and without exogenous FAD (0.3 mM FAD final) added to 1 mg/ml ACAD9 protein and incubated on ice for 30 min before the activity assay.

Limited proteolysis of purified recombinant ACAD9 by trypsin

One hundred µl of 1 mg/ml purified ACAD9 in buffer A was digested with 5 µl of 7 µg/ml of Tosyl phenylalanyl chloromethyl ketone (TPCK)-treated trypsin (ACAD9/trypsin molar ratio of 1000) in the absence and presence of 20-molar excess of exogenous FAD (0.3 mM FAD final). The reaction was incubated at room temperature. At indicated times, aliquots were removed and the reaction was terminated by addition of SDS sample buffer and immediately boiled for 4 min and analyzed by 12.5% SDS–PAGE and stained with Coomassie Blue (Bio-Rad, Hercules, CA, USA).

Molecular modeling

Molecular modeling was performed using *Insight*II software with homology module (Accelyrs, Inc., San Diego, CA, USA) on an SGI Fuel workstation. The atomic coordinates used as template were as published (PDB code 3B96) (18).

Western blotting on mammalian cells

Western blotting of total cell lysates was performed as previously described (51).

Antibodies

Custom-made rabbit polyclonal anti-human ECSIT antibodies were obtained by immunization of purified recombinant ECSIT in rabbits by Cocalico Biologicals (Reamstown, PA, USA). Anti-ACAD9, MCAD, LCAD and VLCAD antisera were produced as already reported (11,27).

ACAD9 activity measurement

ACAD9 activity was measured using palmitoyl-CoA as substrate with the electron transfer flavoprotein fluorescence reduction assay using 100–150 µg protein as described (48,49).

Whole-cell fatty acid oxidation analysis

Whole-cell long-chain FAO was evaluated using a tritium release assay with ^{3}H-palmitate-BSA as the substrate, essentially as described (52). Octanoate oxidation was measured using 125 µM ^{14}C-octanoate under the same conditions, only with substrate oxidation detected through capture of $^{14}CO_2$ following acidification of the media with perchloric acid.

Preparation of mitochondria from cells, BNGE and CI *in situ* activity and staining were performed as previously reported (53).

Complementation of the *ACAD9* –/– HEK293 clone A

ACAD9 knockout HEK293 clone A cells were stably transfected with the mammalian expression vector pcDNA3.1(+) (Invitrogen, Grand Island, NY, USA) containing the normal human *ACAD9* sequence with the mitochondrial precursor (11). Briefly, 1–4 × 10^5 HEK293 clone A cells were plated in a 12-well plate containing 1 ml/well of DMEM and 10% FBS (v/v) but no antibiotics. The next day, cells were transfected with a mixture of 1.6 µg of the *ACAD9* expression vector (or pcDNA3.1 vector as negative control), lipofectamine and Opti-MEM, according to the manufacturer. Selection with G418 (Roche, Boulogne-Billancourt, France) was used at 1 mg/ml for 2–3 weeks. Maintenance concentrations of 0.4 mg/ml G418 were used for further experiments.

Confocal imaging of HEK293 cells

HEK293 (clone A transfected with *ACAD9* expression vector or empty vector) cells were seeded at a concentration of 1 × 10^4 cells/ml on tissue culture-treated glass cover slips and allowed

to grow overnight at 37°C in a 5% CO_2, 95% humidity incubator. Confocal imaging was performed using anti-ACAD9 and anti-cytochrome c oxidase subunit 4 antibody (Abcam, Cambridge, MA, USA) as described previously (54).

Studies with mouse fibroblasts

Acadl/Acadvl double-knockout mouse fibroblasts, deficient in LCAD and VLCAD, were obtained from Dr Keith Cox (15). These cells, generated from skin biopsies taken from double-knockout mice immediately after birth, were cultured in standard conditions. Immunoblotting, enzyme assays and BN gels were performed as described earlier.

Statistical analysis

All statistical comparisons were done by Student's *t*-test, and the corresponding *P* values are provided in the figure legends.

Supplementary Material

Supplementary Material is available at *HMG* online.

Acknowledgements

We thank the staff from the Core Flow Cytometry Laboratory from the University of Pittsburgh, Children's Hospital of UPMC for help with FACS.

Conflict of Interest statement. None declared.

Funding

This study was partly supported by PHS grants NIH R01 DK78775 (J.V.), NIH grant R01 DK090242 (E.S.G.), NIH grant GM29076 (J.J.K.), Children's Hospital of Pittsburgh of UPMC Research Advisory Committee (M.S.), the Philippe Foundation (M.S.) and Société Française de Pédiatrie (M.S.). H.P. was supported by a German Federal Ministry of Education and Research (BMBF, Bonn, Germany) grant to the German Network for Mitochondrial Disorders (mitoNET, 01GM1113C) and the E-RARE project GENOMIT (01GM1207). R.W.T. was supported by a Wellcome Trust Strategic Award (096919/Z/11/Z).

References

1. Swigonova, Z., Mohsen, A.W. and Vockley, J. (2009) Acyl-CoA dehydrogenases: dynamic history of protein family evolution. *J. Mol. Evol.*, **69**, 176–193.
2. He, M., Rutledge, S.L., Kelly, D.R., Palmer, C.A., Murdoch, G., Majumder, N., Nicholls, R.D., Pei, Z., Watkins, P.A. and Vockley, J. (2007) A new genetic disorder in mitochondrial fatty acid beta-oxidation: ACAD9 deficiency. *Am. J. Hum. Genet.*, **81**, 87–103.
3. Haack, T.B., Danhauser, K., Haberberger, B., Hoser, J., Strecker, V., Boehm, D., Uziel, G., Lamantea, E., Invernizzi, F., Poulton, J. *et al.* (2010) Exome sequencing identifies ACAD9 mutations as a cause of complex I deficiency. *Nat. Genet.*, **42**, 1131–1134.
4. Gerards, M., van den Bosch, B.J., Danhauser, K., Serre, V., van Weeghel, M., Wanders, R.J., Nicolaes, G.A., Sluiter, W., Schoonderwoerd, K., Scholte, H.R. *et al.* (2011) Riboflavin-responsive oxidative phosphorylation complex I deficiency caused by defective ACAD9: new function for an old gene. *Brain*, **134**, 210–219.
5. Nouws, J., Nijtmans, L., Houten, S.M., van den Brand, M., Huynen, M., Venselaar, H., Hoefs, S., Gloerich, J., Kronick, J., Hutchin, T. *et al.* (2010) Acyl-CoA dehydrogenase 9 is required for the biogenesis of oxidative phosphorylation complex I. *Cell. Metab.*, **12**, 283–294.
6. Haack, T.B., Madignier, F., Herzer, M., Lamantea, E., Danhauser, K., Invernizzi, F., Koch, J., Freitag, M., Drost, R., Hillier, I. *et al.* (2012) Mutation screening of 75 candidate genes in 152 complex I deficiency cases identifies pathogenic variants in 16 genes including NDUFB9. *J. Med. Genet.*, **49**, 83–89.
7. Calvo, S.E., Compton, A.G., Hershman, S.G., Lim, S.C., Lieber, D.S., Tucker, E.J., Laskowski, A., Garone, C., Liu, S., Jaffe, D.B. *et al.* (2012) Molecular diagnosis of infantile mitochondrial disease with targeted next-generation sequencing. *Sci. Transl. Med.*, **4**, 118ra110.
8. Garone, C., Donati, M.A., Sacchini, M., Garcia-Diaz, B., Bruno, C., Calvo, S., Mootha, V.K. and Dimauro, S. (2013) Mitochondrial encephalomyopathy due to a novel mutation in ACAD9. *JAMA Neurol.*, **70**, 1177–1179.
9. Nouws, J., Wibrand, F., van den Brand, M., Venselaar, H., Duno, M., Lund, A.M., Trautner, S., Nijtmans, L. and Ostergard, E. (2014) A patient with complex I deficiency caused by a novel ACAD9 mutation not responding to riboflavin treatment. *JIMD Rep.*, **12**, 37–45.
10. Haack, T.B., Haberberger, B., Frisch, E.M., Wieland, T., Iuso, A., Gorza, M., Strecker, V., Graf, E., Mayr, J.A., Herberg, U. *et al.* (2012) Molecular diagnosis in mitochondrial complex I deficiency using exome sequencing. *J. Med. Genet.*, **49**, 277–283.
11. Ensenauer, R., He, M., Willard, J.M., Goetzman, E.S., Corydon, T.J., Vandahl, B.B., Mohsen, A.W., Isaya, G. and Vockley, J. (2005) Human acyl-CoA dehydrogenase-9 plays a novel role in the mitochondrial beta-oxidation of unsaturated fatty acids. *J. Biol. Chem.*, **280**, 32309–32316.
12. Nouws, J., Te Brinke, H., Nijtmans, L.G. and Houten, S.M. (2014) ACAD9, a complex I assembly factor with a moonlighting function in fatty acid oxidation deficiencies. *Hum. Mol. Genet.*, **23**, 1311–1319.
13. Shaw, G., Morse, S., Ararat, M. and Graham, F.L. (2002) Preferential transformation of human neuronal cells by human adenoviruses and the origin of HEK 293 cells. *FASEB J.*, **16**, 869–871.
14. Thomas, P. and Smart, T.G. (2005) HEK293 cell line: a vehicle for the expression of recombinant proteins. *J. Pharmacol. Toxicol. Methods*, **51**, 187–200.
15. Cox, K.B., Hamm, D.A., Millington, D.S., Matern, D., Vockley, J., Rinaldo, P., Pinkert, C.A., Rhead, W.J., Lindsey, J.R. and Wood, P.A. (2001) Gestational, pathologic and biochemical differences between very long-chain acyl-CoA dehydrogenase deficiency and long-chain acyl-CoA dehydrogenase deficiency in the mouse. *Hum. Mol. Genet.*, **10**, 2069–2077.
16. Izai, K., Uchida, Y., Orii, T., Yamamoto, S. and Hashimoto, T. (1992) Novel fatty acid beta-oxidation enzymes in rat liver mitochondria. I. Purification and properties of very-long-chain acyl-coenzyme A dehydrogenase. *J. Biol. Chem.*, **267**, 1027–1033.
17. Souri, M., Aoyama, T., Hoganson, G. and Hashimoto, T. (1998) Very-long-chain acyl-CoA dehydrogenase subunit assembles to the dimer form on mitochondrial inner membrane. *FEBS Lett.*, **426**, 187–190.
18. McAndrew, R.P., Wang, Y., Mohsen, A.W., He, M., Vockley, J. and Kim, J.J. (2008) Structural basis for substrate fatty acyl

chain specificity: crystal structure of human very-long-chain acyl-CoA dehydrogenase. *J. Biol. Chem.*, **283**, 9435–9443.
19. Scriver, C.R. and Waters, P.J. (1999) Monogenic traits are not simple: lessons from phenylketonuria. *Trends Genet.*, **15**, 267–272.
20. Okano, Y., Eisensmith, R.C., Guttler, F., Lichter-Konecki, U., Konecki, D.S., Trefz, F.K., Dasovich, M., Wang, T., Henriksen, K., Lou, H. *et al.* (1991) Molecular basis of phenotypic heterogeneity in phenylketonuria. *N. Engl. J. Med.*, **324**, 1232–1238.
21. Distelmaier, F., Koopman, W.J., van den Heuvel, L.P., Rodenburg, R.J., Mayatepek, E., Willems, P.H. and Smeitink, J.A. (2009) Mitochondrial complex I deficiency: from organelle dysfunction to clinical disease. *Brain*, **132**, 833–842.
22. Kevelam, S.H., Rodenburg, R.J., Wolf, N.I., Ferreira, P., Lunsing, R.J., Nijtmans, L.G., Mitchell, A., Arroyo, H.A., Rating, D., Vanderver, A. *et al.* (2013) NUBPL mutations in patients with complex I deficiency and a distinct MRI pattern. *Neurology*, **80**, 1577–1583.
23. Koene, S., Rodenburg, R.J., van der Knaap, M.S., Willemsen, M. A., Sperl, W., Laugel, V., Ostergaard, E., Tarnopolsky, M., Martin, M.A., Nesbitt, V. *et al.* (2012) Natural disease course and genotype-phenotype correlations in Complex I deficiency caused by nuclear gene defects: what we learned from 130 cases. *J. Inherit. Metab. Dis.*, **35**, 737–747.
24. Oey, N.A., Ruiter, J.P., Ijlst, L., Attie-Bitach, T., Vekemans, M., Wanders, R.J. and Wijburg, F.A. (2006) Acyl-CoA dehydrogenase 9 (ACAD 9) is the long-chain acyl-CoA dehydrogenase in human embryonic and fetal brain. *Biochem. Biophys. Res. Commun.*, **346**, 33–37.
25. Oey, N.A., den Boer, M.E., Wijburg, F.A., Vekemans, M., Auge, J., Steiner, C., Wanders, R.J., Waterham, H.R., Ruiter, J.P. and Attie-Bitach, T. (2005) Long-chain fatty acid oxidation during early human development. *Pediatr. Res.*, **57**, 755–759.
26. Spiekerkoetter, U. (2010) Mitochondrial fatty acid oxidation disorders: clinical presentation of long-chain fatty acid oxidation defects before and after newborn screening. *J. Inherit. Metab. Dis.*, **33**, 527–532.
27. Goetzman, E.S., Wang, Y., He, M., Mohsen, A.W., Ninness, B.K. and Vockley, J. (2007) Expression and characterization of mutations in human very long-chain acyl-CoA dehydrogenase using a prokaryotic system. *Mol. Genet. Metab.*, **91**, 138–147.
28. Wang, Y., Mohsen, A.W., Mihalik, S.J., Goetzman, E.S. and Vockley, J. (2010) Evidence for physical association of mitochondrial fatty acid oxidation and oxidative phosphorylation complexes. *J. Biol. Chem.*, **285**, 29834–29841.
29. Heide, H., Bleier, L., Steger, M., Ackermann, J., Drose, S., Schwamb, B., Zornig, M., Reichert, A.S., Koch, I., Wittig, I. *et al.* (2012) Complexome profiling identifies TMEM126B as a component of the mitochondrial complex I assembly complex. *Cell Metab.*, **16**, 538–549.
30. Vockley, J., Parimoo, B. and Tanaka, K. (1991) Molecular characterization of four different classes of mutations in the isovaleryl-CoA dehydrogenase gene responsible for isovaleric acidemia. *Am. J. Hum. Genet.*, **49**, 147–157.
31. Mohsen, A.W., Anderson, B.D., Volchenboum, S.L., Battaile, K. P., Tiffany, K., Roberts, D., Kim, J.J. and Vockley, J. (1998) Characterization of molecular defects in isovaleryl-CoA dehydrogenase in patients with isovaleric acidemia. *Biochemistry*, **37**, 10325–10335.
32. Mathur, A., Sims, H.F., Gopalakrishnan, D., Gibson, B., Rinaldo, P., Vockley, J., Hug, G. and Strauss, A.W. (1999) Molecular heterogeneity in very-long-chain acyl-CoA dehydrogenase deficiency causing pediatric cardiomyopathy and sudden death. *Circulation*, **99**, 1337–1343.
33. Gibson, K.M., Burlingame, T.G., Hogema, B., Jakobs, C., Schutgens, R.B., Millington, D., Roe, C.R., Roe, D.S., Sweetman, L., Steiner, R.D. *et al.* (2000) 2-Methylbutyryl-coenzyme A dehydrogenase deficiency: a new inborn error of L-isoleucine metabolism. *Pediatr. Res.*, **47**, 830–833.
34. Nguyen, T.V., Andresen, B.S., Corydon, T.J., Ghisla, S., Abd-El Razik, N., Mohsen, A.W., Cederbaum, S.D., Roe, D.S., Roe, C. R., Lench, N.J. *et al.* (2002) Identification of isobutyryl-CoA dehydrogenase and its deficiency in humans. *Mol. Genet. Metab.*, **77**, 68–79.
35. Nguyen, T.V., Riggs, C., Babovic-Vuksanovic, D., Kim, Y.S., Carpenter, J.F., Burghardt, T.P., Gregersen, N. and Vockley, J. (2002) Purification and characterization of two polymorphic variants of short chain acyl-CoA dehydrogenase reveal reduction of catalytic activity and stability of the Gly185Ser enzyme. *Biochemistry*, **41**, 11126–11133.
36. Pedersen, C.B., Bross, P., Winter, V.S., Corydon, T.J., Bolund, L., Bartlett, K., Vockley, J. and Gregersen, N. (2003) Misfolding, degradation, and aggregation of variant proteins. The molecular pathogenesis of short chain acyl-CoA dehydrogenase (SCAD) deficiency. *J. Biol. Chem.*, **278**, 47449–47458.
37. Vockley, J. and Ensenauer, R. (2006) Isovaleric acidemia: new aspects of genetic and phenotypic heterogeneity. *Am. J. Med. Genet. C Semin. Med. Genet.*, **142C**, 95–103.
38. Gregersen, N., Andresen, B.S., Pedersen, C.B., Olsen, R.K., Corydon, T.J. and Bross, P. (2008) Mitochondrial fatty acid oxidation defects–remaining challenges. *J. Inherit. Metab. Dis.*, **31**, 643–657.
39. Pedersen, C.B., Kolvraa, S., Kolvraa, A., Stenbroen, V., Kjeldsen, M., Ensenauer, R., Tein, I., Matern, D., Rinaldo, P., Vianey-Saban, C. *et al.* (2008) The ACADS gene variation spectrum in 114 patients with short-chain acyl-CoA dehydrogenase (SCAD) deficiency is dominated by missense variations leading to protein misfolding at the cellular level. *Hum. Genet.*, **124**, 43–56.
40. Brown-Harrison, M.C., Nada, M.A., Sprecher, H., Vianey-Saban, C., Farquhar, J. Jr, Gilladoga, A.C. and Roe, C.R. (1996) Very long chain acyl-CoA dehydrogenase deficiency: successful treatment of acute cardiomyopathy. *Biochem. Mol. Med.*, **58**, 59–65.
41. Roe, C.R., Sweetman, L., Roe, D.S., David, F. and Brunengraber, H. (2002) Treatment of cardiomyopathy and rhabdomyolysis in long-chain fat oxidation disorders using an anaplerotic odd-chain triglyceride. *J. Clin. Invest.*, **110**, 259–269.
42. Nagao, M. and Tanaka, K. (1992) FAD-dependent regulation of transcription, translation, post-translational processing, and post-processing stability of various mitochondrial acyl-CoA dehydrogenases and of electron transfer flavoprotein and the site of holoenzyme formation. *J. Biol. Chem.*, **267**, 17925–17932.
43. Zschocke, J. (2012) HSD10 disease: clinical consequences of mutations in the HSD17B10 gene. *J. Inherit. Metab. Dis.*, **35**, 81–89.
44. Rauschenberger, K., Scholer, K., Sass, J.O., Sauer, S., Djuric, Z., Rumig, C., Wolf, N.I., Okun, J.G., Kolker, S., Schwarz, H. *et al.* (2010) A non-enzymatic function of 17beta-hydroxysteroid dehydrogenase type 10 is required for mitochondrial integrity and cell survival. *EMBO Mol. Med.*, **2**, 51–62.
45. Li, C., Chen, P., Palladino, A., Narayan, S., Russell, L.K., Sayed, S., Xiong, G., Chen, J., Stokes, D., Butt, Y.M. *et al.* (2010) Mechanism of hyperinsulinism in short-chain 3-hydroxyacyl-CoA dehydrogenase deficiency involves activation of glutamate dehydrogenase. *J. Biol. Chem.*, **285**, 31806–31818.

46. Runswick, M.J., Fearnley, I.M., Skehel, J.M. and Walker, J.E. (1991) Presence of an acyl carrier protein in NADH:ubiquinone oxidoreductase from bovine heart mitochondria. *FEBS Lett.*, **286**, 121–124.
47. Vafai, S.B. and Mootha, V.K. (2012) Mitochondrial disorders as windows into an ancient organelle. *Nature*, **491**, 374–383.
48. Frerman, F.E. and Goodman, S.I. (1985) Fluorometric assay of acyl-CoA dehydrogenases in normal and mutant human fibroblasts. *Biochem. Med.*, **33**, 38–44.
49. Mohsen, A.W. and Vockley, J. (1995) High-level expression of an altered cDNA encoding human isovaleryl-CoA dehydrogenase in Escherichia coli. *Gene*, **160**, 263–267.
50. Lehman, T.C., Hale, D.E., Bhala, A. and Thorpe, C. (1990) An acyl-coenzyme A dehydrogenase assay utilizing the ferricenium ion. *Anal. Biochem.*, **186**, 280–284.
51. Barbi de Moura, M., Uppala, R., Zhang, Y., Van Houten, B. and Goetzman, E.S. (2014) Overexpression of mitochondrial sirtuins alters glycolysis and mitochondrial function in HEK293 cells. *PLoS One*, **9**, e106028.
52. Rardin, M.J., He, W., Nishida, Y., Newman, J.C., Carrico, C., Danielson, S.R., Guo, A., Gut, P., Sahu, A.K., Li, B. *et al.* (2013) SIRT5 regulates the mitochondrial lysine succinylome and metabolic networks. *Cell Metab.*, **18**, 920–933.
53. Graves, J.A., Wang, Y., Sims-Lucas, S., Cherok, E., Rothermund, K., Branca, M.F., Elster, J., Beer-Stolz, D., Van Houten, B., Vockley, J. *et al.* (2012) Mitochondrial structure, function and dynamics are temporally controlled by c-Myc. *PLoS One*, **7**, e37699.
54. Schiff, M., Mohsen, A.W., Karunanidhi, A., McCracken, E., Yeasted, R. and Vockley, J. (2013) Molecular and cellular pathology of very-long-chain acyl-CoA dehydrogenase deficiency. *Mol. Genet. Metab.*, **109**, 21–27.